Distinct fusion properties of synaptotagmin-1 and synaptotagmin-7 bearing dense core granules

Tejeshwar C. Rao[a], Daniel R. Passmore[a], Andrew R. Peleman[a], Madhurima Das[a], Edwin R. Chapman[b], and Arun Anantharam[a]

[a]Department of Biological Sciences, Wayne State University, Detroit, MI 48202; [b]Howard Hughes Medical Institute, Department of Neuroscience, University of Wisconsin, Madison, WI 53705

ABSTRACT **Adrenal chromaffin cells release hormones and neuropeptides that are essential for physiological homeostasis. During this process, secretory granules fuse with the plasma membrane and deliver their cargo to the extracellular space. It was once believed that fusion was the final regulated step in exocytosis, resulting in uniform and total release of granule cargo. Recent evidence argues for nonuniform outcomes after fusion, in which cargo is released with variable kinetics and selectivity. The goal of this study was to identify factors that contribute to the different outcomes, with a focus on the Ca^{2+}-sensing synaptotagmin (Syt) proteins. Two Syt isoforms are expressed in chromaffin cells: Syt-1 and Syt-7. We find that overexpressed and endogenous Syt isoforms are usually sorted to separate secretory granules and are differentially activated by depolarizing stimuli. In addition, overexpressed Syt-1 and Syt-7 impose distinct effects on fusion pore expansion and granule cargo release. Syt-7 pores usually fail to expand (or reseal), slowing the dispersal of lumenal cargo proteins and granule membrane proteins. On the other hand, Syt-1 diffuses from fusion sites and promotes the release of lumenal cargo proteins. These findings suggest one way in which chromaffin cells may regulate cargo release is via differential activation of synaptotagmin isoforms.**

Monitoring Editor
Adam Linstedt
Carnegie Mellon University

Received: Feb 3, 2014
Revised: Jun 9, 2014
Accepted: Jun 11, 2014

INTRODUCTION

It was once believed that exocytosis occurred in an all-or-none manner, in which, after a secretory granule fused, it was committed to release all of its contents. More recent evidence suggests that in the adrenal chromaffin cell, mechanisms have evolved to regulate content release after fusion by controlling the rate or the extent of fusion pore expansion (Taraska *et al.*, 2003; Taraska and Almers, 2004; Perrais *et al.*, 2004; Fulop *et al.*, 2005, 2008; Anantharam *et al.*, 2011). The fusion pore is the aqueous passage through which essential signaling molecules (neurotransmitters, hormones, neuropeptides, etc.) are expelled into the extracellular space. Control over the sieving properties of the fusion pore greatly expands the physiological range of exocytosis. It allows, for example, cells to release contents selectively on the basis of size exclusion; smaller hormones leave small pores more readily than larger proteins, which are retained. Such selective content release may be relevant to different functions of the adrenal medulla as part of the sympathetic nervous system. Under basal conditions, chromaffin cells release catecholamines (epinephrine and norepinephrine) at a low basal rate set by the sympathetic tone (de Diego *et al.*, 2008). Basal secretion is linked with the cavicapture fusion mode, in which granules fuse and release contents through a transient opening, which reseals (Taraska *et al.*, 2003; Perrais *et al.*, 2004). Acute stress dramatically up-regulates not only the level of catecholamines in the circulation, but also a variety of neuropeptides with roles in the peripheral response (Damase-Michel *et al.*, 1993; Edwards and Jones, 1993; de Diego *et al.*, 2008). The increased sympathetic activation of the adrenal medulla during stress is linked with full-collapse fusion. In this mode, the pore expands widely, allowing for more thorough release of granule lumen constituents. Despite these observations, there is a gap in our knowledge with respect to the molecular events that regulate fusion

This article was published online ahead of print in MBoC in Press (http://www.molbiolcell.org/cgi/doi/10.1091/mbc.E14-02-0702) on June 18, 2014.

Address correspondence to: Arun Anantharam (anantharam@wayne.edu).

Abbreviations used: A.F.U., arbitrary fluorescence units; CgB, chromogranin B; diD, 1,1′-dioctadecyl-3,3,3′,3′-tetramethylindodicarbocyanine, 4-chlorobenzenesulfonate salt; NPY, neuropeptide-Y; *P+2S*, (*p*-pol emission) + 2 (*s*-pol emission); *P/S*, (*p*-pol emission)/(*s*-pol emission); PSS, physiological saline solution; pTIRFM, polarized total internal reflection microscopy; VAMP, vesicle-associated membrane protein.

pore expansion and concomitant content dispersal. Because of the importance of adrenal hormones for physiological homeostasis, this is a major limitation.

In chromaffin cells, the trigger for stimulus-evoked exocytosis is a rise in intracellular Ca^{2+}. The level of intracellular Ca^{2+} accumulation varies with the stimulus intensity and secretogogue (Augustine and Neher, 1992; Garcia *et al.*, 2006; de Diego *et al.*, 2008). Ca^{2+} regulates release by acting on the Ca^{2+}-binding synaptotagmin (Syt) protein family (Brose *et al.*, 1992; Voets *et al.*, 2001; Schonn *et al.*, 2008), driving their association with membranes that harbor anionic lipids (Tucker *et al.*, 2004). This interaction between the Syt-Ca^{2+} complex and the membrane is proposed to serve as a critical step in excitation–secretion coupling (Brose *et al.*, 1992). Although there are at least 17 Syt isoforms, chromaffin cells express only two: Syt-1 and Syt-7 (Schonn *et al.*, 2008). The two isoforms differ in their affinity for Ca^{2+} in the presence of anionic phospholipids and their rate of disassociation from phospholipids (Sugita *et al.*, 2002; Tucker *et al.*, 2003; Bhalla *et al.*, 2005; Hui *et al.*, 2005). The goal of the present study was to determine whether the divergent biochemistry of the two Syt isoforms expressed in chromaffin cells imposes functionally divergent effects on dense core granule exocytosis. That the roles of Syt isoforms in chromaffin cells are distinct is suggested by previous studies in the PC12 cell line. PC12s express 4 Syt isoforms: 1, 4, 7, and 9 (Fukuda, 2004; Fukuda *et al.*, 2002, 2004). Overexpression studies suggest that isoforms harbor a size preference for secretory granules (Zhang *et al.*, 2011) and endow the fusion event with different functional and kinetic properties (Moghadam and Jackson, 2013). Syt-4, for example, negatively regulates exocytosis, increasing the probability that pores will reseal after fusion (Wang *et al.*, 2001; Zhang *et al.*, 2011). Syt-1 fusion also produces more cavicapture events than either Syt-7 or Syt-9 (Wang *et al.*, 2001, 2003, 2006; Bai *et al.*, 2004). Suppression of Syt-1 and Syt-9 expression abolishes Ca^{2+}-dependent release, suggesting that these two isoforms account for all regulated exocytosis in PC12 cells (Lynch and Martin, 2007).

In this study, we identify fundamentally different roles for Syt-1 and Syt-7 in chromaffin cell exocytosis. We find that endogenous Syt-1 and Syt-7 rarely colocalize on granules, with most expressing only one isoform or the other. Syt isoform effects on fusion, fusion pore expansion, and endocytosis were also distinct. When overexpressed, Syt-1 enables the rapid expansion of fusion pores and promotes the release of granule membrane and lumenal proteins. On the other hand, Syt-7 fusion pores usually fail to expand (or reseal) and restrict cargo release. Consistent with these results, granules with Syt-1 overwhelmingly undergo the full-collapse mode of fusion, whereas those with Syt-7 exhibit higher rates of endocytosis. Finally, we find that isoforms have different requirements for activation. A more strongly depolarizing stimulus, and a correspondingly greater increase in intracellular Ca^{2+}, is necessary to activate Syt-1 than it is to activate Syt-7. On the basis of these results, we propose that selective, stimulus-dependent activation of the Syt isoforms play an important role in controlling chromaffin cell fusion modes.

RESULTS

Synaptotagmin isoforms are sorted to different granule populations

Chromaffin cells express two protein isoforms of synaptotagmin (Syt-1, Syt-7). An important question is whether they are sorted to the same or separate secretory granules. A recent study in PC12 cells, which express Syt-1, 4, 7, and 9, showed there to be significant differences in isoform sorting (Zhang *et al.*, 2011). Therefore our first goal was to visualize chromaffin cell granules and determine how frequently they express one or both isoforms. We transfected cells with neuropeptide Y–Cerulean (NPY-Cer) to label granules and identified isoforms using antibodies against Syt-1 and Syt-7. We then counted the number of fluorescent Syt-1 and/or Syt-7 puncta that colocalized with NPY. The data are shown in Figure 1, A and B. Across 17 cells, almost 69% of NPY-labeled granules expressed either Syt-1 or Syt-7. Fewer than 20% of NPY granules did not have any Syt-protein, whereas an even smaller number (<10%) expressed both isoforms. We also examined whether overexpression altered the distribution of synaptotagmin resulting in increased colocalization of isoforms on granules. Cells were transfected with NPY-Cer, Syt-1–green fluorescent protein (GFP), and Syt-7–mCherry and analyzed as before. We found that even when overexpressed, synaptotagmin isoforms were usually segregated within cells, with only 9.5% of NPY-Cer granules harboring both Syt-1 and Syt-7 (Supplemental Figure S1A). When overexpressed, the amount of synaptotagmin on granules is approximately two times higher than it is in nontransfected cells (Supplemental Figure S1D).

Many granules expressing synaptotagmins did not express NPY-Cer, which may either reflect inefficiencies inherent in the expression of exogenous proteins via transfection or true heterogeneity in the distribution of NPY across granules. Nonetheless, in the population of granules without NPY-Cer, the colocalization of endogenous Syt-1 and Syt-7 (Figure 1C) or overexpressed Syt-1–GFP and Syt-7–mCherry (Supplemental Figure S1C) remained low. Finally, to verify these results, we stained for endogenous Syt-1 in cells expressing Syt-7–mCherry and endogenous Syt-7 in cells expressing Syt-1–mCherry. As the data in Supplemental Figure S2C show, only a fraction of granules with Syt-7–mCherry harbor endogenous Syt-1, and similarly, only a small number of granules with Syt-1–mCherry harbor endogenous Syt-7. Overall, these experiments demonstrate that Syt-1 and Syt-7 are usually sorted to separate secretory granules—even when overexpressed—with a minority of granules expressing both isoforms.

Stimulation-evoked surface distribution of synaptotagmin isoforms is distinct

We next examined the functional consequences of isoform segregation on secretory granule exocytosis. We reasoned that if Syt isoforms drive different modes of granule fusion in chromaffin cells, as previously reported in PC12 cells (Zhang *et al.*, 2011), their stimulus-evoked appearance on the cell surface should also be distinct. To test this idea, we stimulated cells expressing Syt-1 (wild type [WT]) and c-myc–Syt-7 with 56 mM KCl for 30 s. This treatment depolarizes the membrane potential and triggers exocytosis (Anantharam *et al.*, 2011). Cell activity was rapidly arrested with an ice-cold (4°C) physiological saline solution followed by incubation with a solution of bovine serum albumin (BSA) containing the N-terminal lumenal domain primary antibody to Syt-1 or anti-myc (to bind transfected c-myc–Syt-7). These antibodies recognize portions of the Syts that are exposed to the extracellular solution after granule fusion. The cells were then washed to remove primary antibodies, fixed, and exposed to fluorescent secondary antibodies. The cell footprint (i.e., the part of the cell affixed to the coverglass and observable in the field of view) was subsequently imaged with a total internal reflection fluorescence (TIRF) microscope. The immunocytochemistry revealed that after fusion, most Syt-1 is distributed diffusely along the plasma membrane (Figure 2A). On the other hand, Syt-7 is confined to discrete clusters (puncta) on the plasma membrane (Figure 2A). To verify that the antibody was only binding to surface Syts and not to protein within the cytosol, we used a confocal microscope to visualize the cell interior. As we focused away from the focal plane closest to the coverglass and further into the cell, little fluorescence

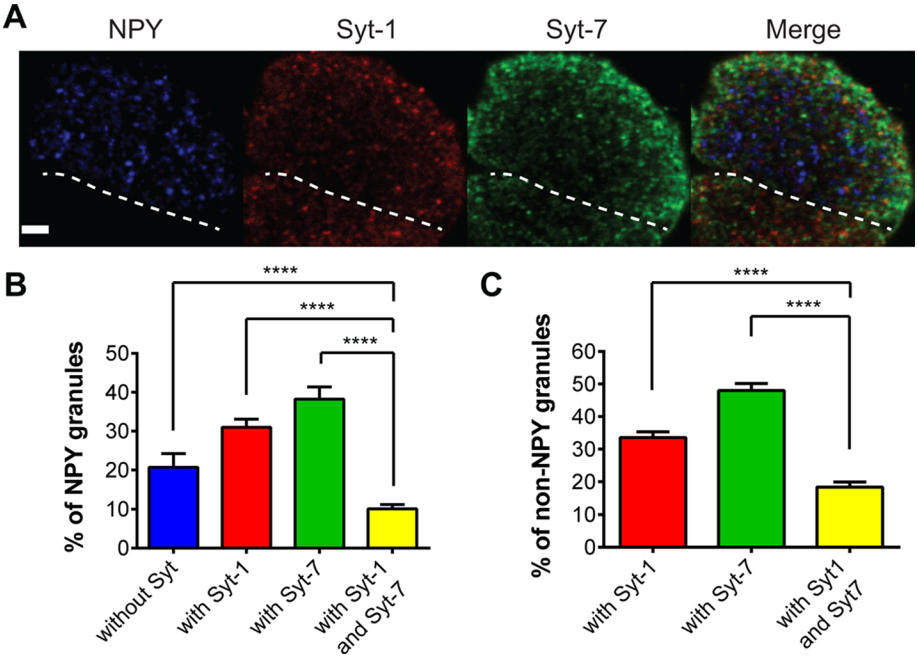

FIGURE 1: Confocal imaging of Syt isoform expression on NPY-containing granules. (A) Chromaffin cells cultured on glass coverslips were transfected with a plasmid encoding NPY-Cer. At 3–4 d after transfection, cells were fixed, permeabilized, and exposed to Syt-1 and Syt-7 antibodies. Confocal sections of 0.5 µm were taken through the cell. The region closest to the coverglass was imaged. The dotted line indicates the boundary of the transfected NPY-Cer cell from a nontransfected cell below. Scale bar, 3 µm. (B) The percentage colocalization of NPY granules with any synaptotagmin or with Syt-1, Syt-7, and Syt-1 plus Syt-7. Differences between groups were assessed with the Student's *t* test ($n = 17$ cells, ****$p < 0.0001$). (C) Synaptotagmin isoforms were sometimes detected in regions without obvious NPY-Cer fluorescence. Colocalization of isoforms in non-NPY granules was determined. Differences between groups were assessed with the Student's *t* test ($n = 17$ cells, ****$p < 0.0001$).

was evident (Supplemental Figure S2C). In the absence of stimulation, there was minimal plasma membrane fluorescence attributable to Syt-1 or Syt-7 when imaged with either the confocal (Supplemental Figure S2C) or TIRF (Figure 2A) microscope.

Syt-1 spreads out of fusion sites, whereas Syt-7 persists at the pore

The clustered surface distribution of Syt-7 could reflect protein confined to a partially open fusion pore or domains of protein aggregation on the plasma membrane after collapse of the granule membrane. To distinguish between these possibilities, we monitored Syt-7–pHluorin (pHluorin is on the N-terminal lumenal domain) intensity changes after fusion, as well as the underlying topology of the fused granule membrane with polarization and total internal reflection fluorescence microscopy (pTIRFM). Transfected cells were labeled with diD, a fluorophore that intercalates in the plasma membrane with its transition dipole moments roughly parallel to the membrane plane. Local perfusion of a 56 mM KCl solution depolarizes the cell membrane and triggers exocytosis. During experiments, cells were sequentially exposed to 488-nm TIR illumination (to excite pHluorin) and 561-nm TIR illumination (to excite diD) that is either *p* or *s* polarized. Details on how the polarizations are generated are given elsewhere (Anantharam *et al.*, 2010). From the *P* and *S* emissions, we calculated pixel-to-pixel *P/S* and *P* + *2S* images. The *P/S* images report on diD-labeled membrane curvature. *P/S* is expected to increase immediately upon granule fusion as diD diffuses from the plasma membrane into the granule membrane. Its decay over time reflects the rate of granule membrane collapse into the plasma membrane. *P* + *2S* reports on total diD emission. Computer simulations indicate that *P* + *2S* will increase if the geometry results in more diD-labeled membrane close to the glass interface, as when a fused granule is attached to the plasma membrane by a neck. *P* + *2S* will decrease if diD diffuses into a postfusion membrane indentation (placing diD farther from the substrate and thereby in a dimmer evanescent field intensity). Thus together *P/S* and *P* + *2S* provide information on the changing geometry of the fusion pore as it expands, reseals, or remains stable (Anantharam *et al.*, 2010).

Using this approach, we found that Syt-7 remains clustered after fusion (Figure 3A) at indentations whose *P/S* and *P* + *2S* emissions are consistent with a granule connected to the plasma membrane via a short neck (Figure 3E; Anantharam *et al.*, 2010, 2011). Spreading of Syt-7 out of these indentations is restricted, suggesting that the protein is anchored to structures in either the membrane or the cytoplasm. To determine how long Syt-7 was on the cell surface and exposed to the extracellular space, we stimulated cells expressing Syt-7–pHluorin for 30 s, followed by periodic washes with physiological salt solution (PSS) at pH 7.4 and 5.5 (Figure 3, B–D, black bars). This treatment quenches the pHluorin fluorescence (Figure 3B). Because diD is also pH sensitive, *P* + *2S* emission diminishes during the pH 5.5 washes (Figure 3D).

Overall, the pH switching method revealed that 71% (36 of 51 events; six cells) of Syt-7 fusion pores were accessible to the extracellular space for at least 40 s. For some Syt-7 fusion events (15 of 51 events), the pHluorin signal is evident but suddenly no longer quenched by low pH—consistent with endocytosis having occurred. An example of an endocytic event is shown in Figure 4. Before stimulation with 56 mM KCl, no Syt-7 pHluorin fluorescence is evident either within the circled region or at the arrow (Figure 4A). On depolarization, fluorescent spots suddenly appear as the granule lumen is exposed to the neutral extracellular pH. Subsequent washes with a pH 5.5 solution reveal that one of the spots is insensitive to quenching (within the circled region in Figure 4A and graph in Figure 4B). The granule within the circled region has most likely undergone endocytosis at the site of fusion. Measurements of membrane topology independently support this conclusion (Figure 4, C and D). Both *P/S* and *P* + *2S* increase as the granule and plasma membranes fuse. Periodic dips in *P* + *2S* are observed during low-pH application, but after accounting for photobleaching, the trend is for *P* + *2S* at fusion sites to remain elevated (Figure 4D). *P/S* does not change in response to low pH because the *P* and *S* emissions are reduced proportionately (Figure 4C). Computer simulations predict that the persistent increases in *P/S* and *P* + *2S* are most consistent with a diD-labeled endocytosed membrane remaining within the evanescent field after fusion (Figure 4E). This is independently supported by the insensitivity of the pHluorin signal to low-pH perfusion.

Conversely, Syt-1-pHluorin diffuses from sites of granule fusion. One example of this is shown in Figure 5, A and B. The spreading

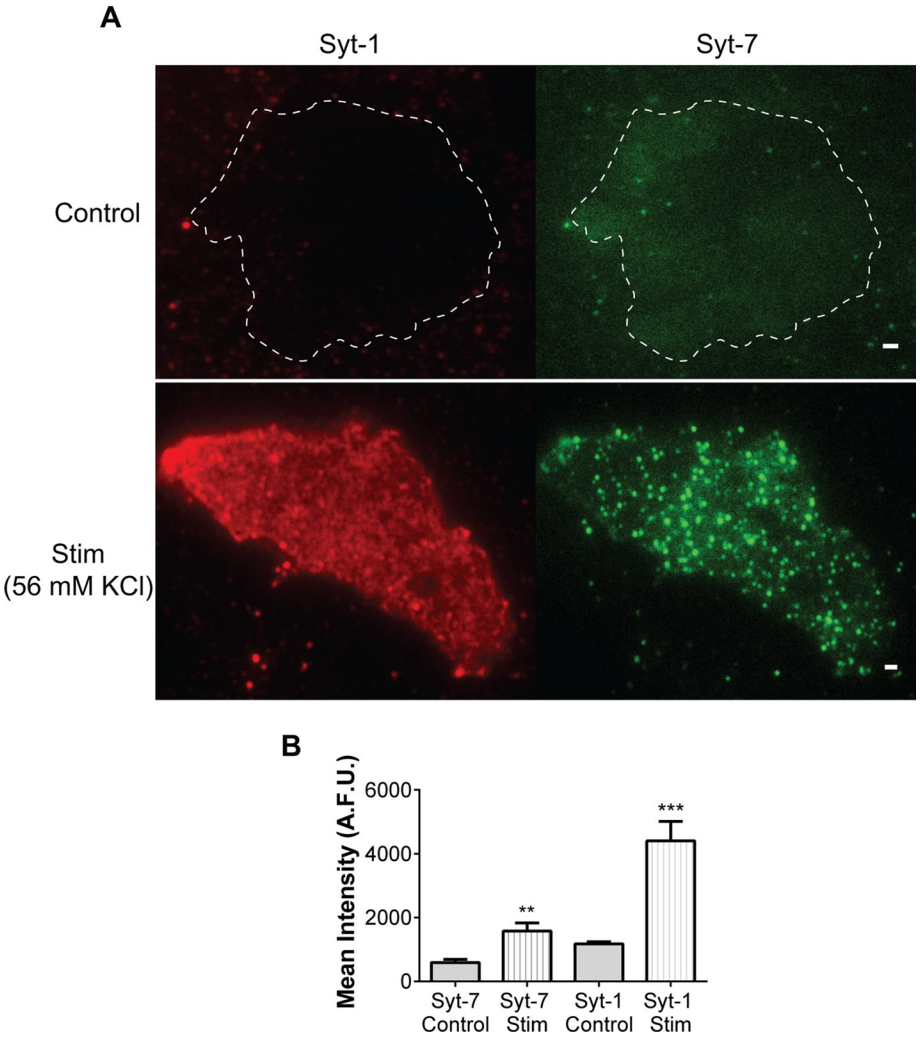

FIGURE 2: Chromaffin cells were exposed to physiological saline solution (control) or 56 mM KCl PSS for 30 s. Cell activity was arrested with ice-cold saline solution. The cells were then incubated with N-terminal lumenal domain antibody to Syt-1 or anti-myc (recognizes transfected c-myc–Syt-7), stained with fluorescent secondary antibodies, and imaged with a TIRF microscope. (A) In the absence of stimulation, little surface Syt fluorescence is visible. Top, dotted white line is the membrane outline of the imaged cell. With stimulation, Syt-7 appears on the surface with a punctate distribution, whereas Syt-1 distribution is more diffuse. (B) Quantification of the entire cell footprint (i.e., the part of the cell adhered to the coverglass and imaged) of control (unstimulated) and ctimulated (Stim) cells expressing Syt-1 WT or c-myc Syt-7 (from six cells). Data are averages ± SEM (**$p < 0.01$, ***$p < 0.001$, Student's t test). Surface intensity increased by 2.7 times for stimulated Syt-7 cells and 3.7 times for stimulated Syt-1 cells.

fluorescence of Syt-1 in the plane of the plasma membrane was further analyzed by calculating the diffusion coefficient (D) for a subset of events. D was calculated from the slope of the plot of w^2 versus time, where w^2 is the variance of the Gaussian fit of the Syt-1 fluorescence (Figure 5C). The diffusion coefficient for the event shown in Figure 5A was calculated to be 0.53×10^{-2} μm^2/s. The mean diffusion coefficient from 17 Syt-1 fusion events with approximately linear increases in w^2 versus time was calculated as $0.63 \times 10^{-2} \pm 0.15$ μm^2/s. This value is more than an order of magnitude smaller than that calculated for vesicular monoamine transporter (VAMP) in chromaffin cells (Allersma *et al.*, 2004). This suggests that even when Syt-1 diffuses out of fusion sites, it does so slowly. Only 8% (3 of 36) of Syt-1 pHluorin fusion events are punctate for 40 s or more.

Postfusion topological changes are associated with distinct fusion modes for Syt-1 and Syt-7 granules

Averaged pHluorin intensities show that whereas Syt-1 disperses from fusion sites, Syt-7 tends to stay clustered (Figure 6A). Measurements of endocytic frequency and membrane topological changes suggest fundamentally different outcomes for Syt-1 and Syt-7 after fusion (Figure 6, A–D). Postfusion *P/S* signals (representing the indented fused granule/plasma membrane domain) decay to baseline within 5 s for the majority of Syt-1 events (27 of 36 events, or 75%; Figure 6C). Meanwhile, 82% (42 of 51 events) of Syt-7 postfusion indentations persist (i.e., show no evidence of decay or collapse) for the duration of the imaging period. This ranged from 40 to ~80 s, depending on when the granule fused with respect to time of stimulus application. For 31 granules that fused soon after the stimulus was applied, the indentations (*P/S* increase) lasted for at least 80 s. This stands in stark contrast to Syt-1 postfusion indentations, which lasted for the duration of the imaging period in only three of 36 cases. Topological changes were also monitored during fusion of vesicular monoamine transporter-2 (VMAT-2) pHluorin–expressing granules. These events exhibit an intermediate phenotype, with 38% (nine of 24) of *P/S* signals decaying to baseline within 5 s (Supplemental Figure S3B). This is not surprising, as ostensibly VMAT-2 is expressed on Syt-1 and Syt-7 granules.

Most fusion events with a *P/S* change were also accompanied by a change in *P + 2S*, which indicates total diD emission from a region of interest. This was true for 37 of 51 Syt-7 events, 23 of 36 Syt-1 events (Figure 6D), and 17 of 24 VMAT-2 events (Supplemental Figure S3C). *P + 2S* changes associated with Syt-1 granule fusion were overwhelmingly short lived. In only one instance did a *P + 2S* change persist for >5 s. When observed, *P + 2S* also tended to decrease rather than increase, suggesting a widening pore. In contrast, at sites of Syt-7 fusion, *P + 2S* usually increased (34 of 37) rather than decreased (3 of 37), with most lasting for >5 s. *P + 2S* changes after VMAT-2 granule fusion were again intermediate, with roughly equivalent numbers of events associated with increases and decreases (Supplemental Figure S3C).

Thus fusion of Syt-7 granules results in the formation of a pore that frequently reseals, resulting in endocytosis (29% of events). The remaining 71% of events may either be progressing to cavicapture or, alternatively, full-collapse fusion with slower kinetics. In contrast, Syt-1 pores expand widely after fusion. A small minority of these fusion events end in endocytosis (8% of events; Figure 6B). When a much larger number of events is considered—that is, from cells expressing Syt-1 or Syt-7 pHluorin but not stained

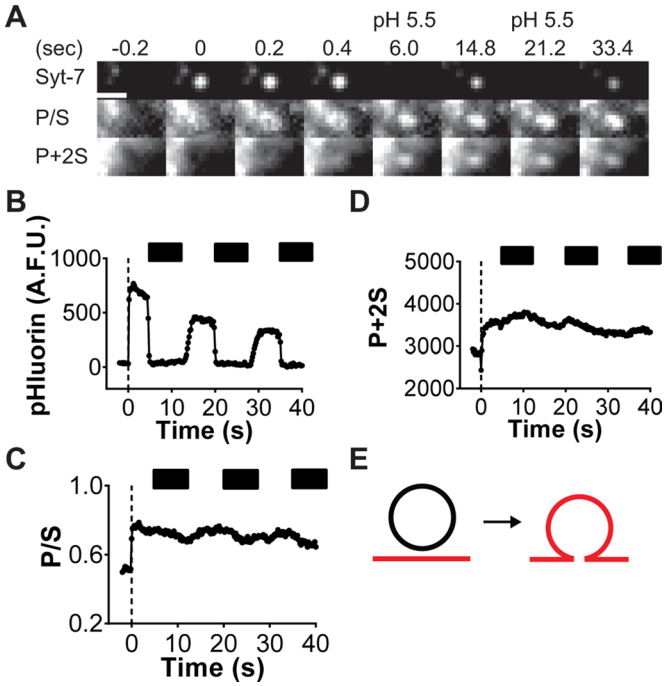

FIGURE 3: Syt-7 fluorescence persists at sites of fusion for tens of seconds. (A) The fusion of a Syt-7–pHluorin granule and concomitant increases in diD-labeled membrane curvature (*P/S*) and concentration (*P + 2S*). Scale, 960 nm. (B–D) Intensity vs. time for images in A. Dotted line at time 0 indicates the prefusion. Black bars indicate duration of pH 5.5 PSS washes. (E) Based on computer simulations (as described in Anantharam *et al.* (2010), the increases in *P/S* and *P + 2S* are consistent with a fusion pore that fails to expand.

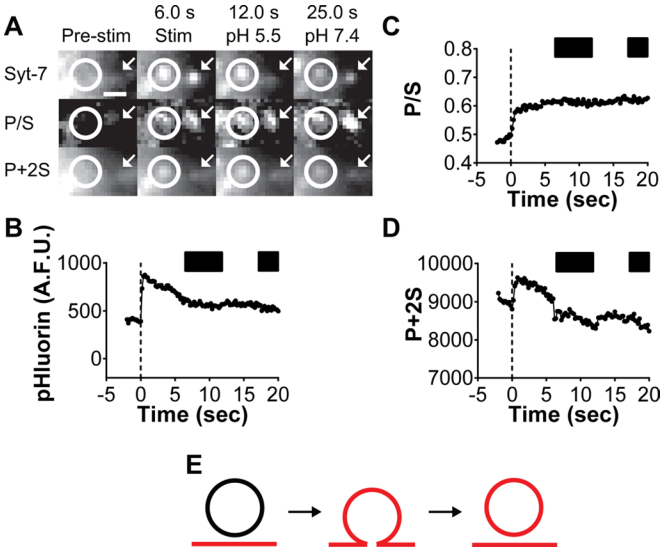

FIGURE 4: Fusion of Syt-7 granules sometimes results in cavicapture. (A) Two Syt-7 pHluorin fusion events (circle and arrow). Before fusion (Pre-stim) no fluorescence is visible at either site. With stimulation (6.0 s), puncta are evident within the circled region and at the arrow. Syt-7 fluorescence within the circled region is not quenched by pH 5.5 PSS, suggesting that this event has undergone endocytosis at the site of fusion (cavicapture). Syt-7 fluorescence at the arrow is sensitive to a wash of pH 5.5 PSS, suggesting that the granule lumen is accessible to the extracellular space via a pore. Scale, 960 nm. (B–D) Graphs for pHluorin, *P/S*, and *P + 2S* emission images within circled region of A. (E) The emission intensity changes observed are consistent with an endocytosed membrane remaining within the evanescent field, yielding increases in *P/S* and *P + 2S*.

with diD—the frequency of endocytosis remains considerably lower for Syt-1 than for Syt-7. Three of 289 Syt-1 fusion events resulted in endocytosis versus 68 of 310 Syt-7 fusion events (Supplemental Figure S3D). This demonstrates that diD staining did not, on its own, change the prevailing fusion mode for Syt-1 and Syt-7 granules.

Syt-7 slows dispersal of granule cargo proteins and membrane proteins

The topological changes observed in Figure 6 demonstrate that Syt-7 fusion pores widen slowly (or reseal), whereas Syt-1 pores expand widely. If the presence of Syt-7 on the granule retards pore expansion, the dispersal of lumenal granule contents should also be slowed. To determine whether this was the case, we transfected cells to express Syt-1 or Syt-7-mCherry and chromogranin B (CgB) pHluorin. We monitored the release of CgB out of granules with either Syt-1 or Syt-7. Representative CgB-pHluorin release events from Syt-1 and Syt-7 granule are shown in Figure 7, A–D. On average, CgB release from Syt-1 granules (circles in graph) occurred more rapidly than from Syt-7 granules (squares in graph).

We also studied the effects of Syt-7 expression on the diffusion of a granule membrane protein, VMAT-2, out of the fused granule/plasma membrane domain. VMAT2-pHluorin ordinarily diffuses rapidly from sites of Syt-1 granule fusion, exhibiting a roughly twofold higher diffusion coefficient than Syt-1 (Figure 8, A and B, and Supplemental Figure S3D). However, when VMAT-2 is coexpressed with Syt-7, its movement out of fusion sites is significantly disrupted (Figure 8, C and D). Indeed, VMAT-2 fluorescence shows a strong tendency to persist at the fusion site along with Syt-7. The postfusion fluorescence intensity from many fusion events is shown in Figure 8E. Fluorescence intensity decays to baseline in roughly 4 s for VMAT-2 + Syt-1 events, whereas it is resistant to decay in the case of VMAT-2 + Syt-7 events.

Synaptotagmins are differentially activated by depolarizing stimuli

Membrane depolarization opens voltage-gated channels, allowing Ca^{2+} to accumulate within cells and trigger exocytosis. The level of

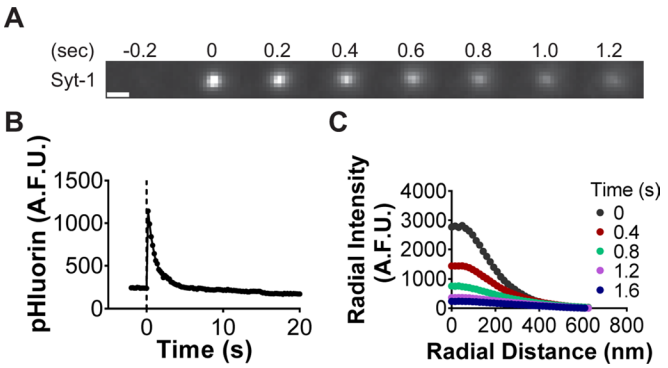

FIGURE 5: Syt-1 diffusion. (A) Syt-1-pHluorin diffusing from a fusion site. Scale, 960 nm. (B) Syt-1-pHluorin intensity decay. (C) The diffusion coefficient (*D*) of Syt-1 was calculated from the variance (w^2) vs. time of Gaussian fits by using $D = \Delta w^2/4\Delta t$. The diffusion coefficient for the Syt-1 fusion event shown was calculated to be 0.53×10^{-2} μm²/s. For clarity, radial intensity profiles every 400 ms are shown (images were actually acquired at 5 Hz).

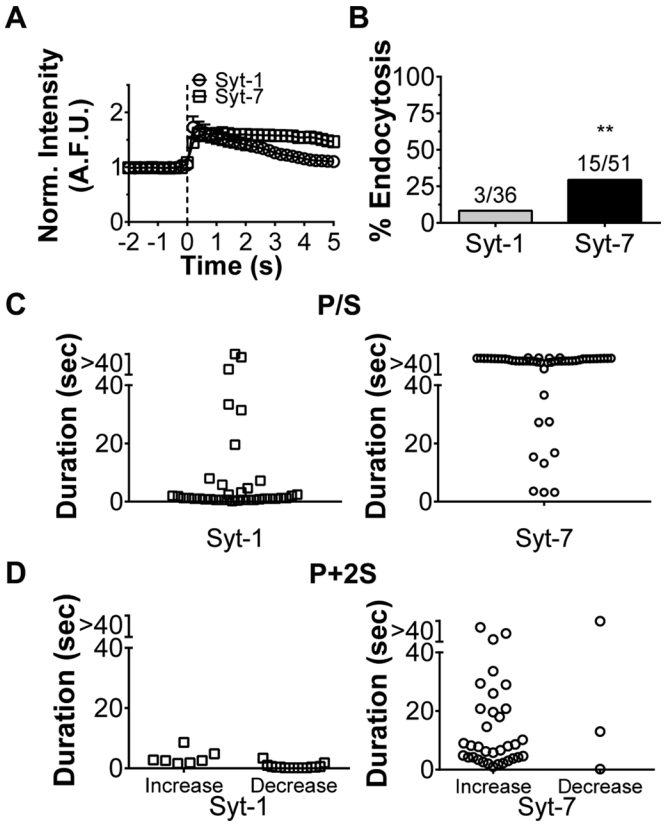

FIGURE 6: (A) Averaged, normalized intensities of Syt-1 ($n = 36$; seven cells) and Syt-7 ($n = 51$; six cells) fusion events ± SEM. Means are significantly different after 2.8 s (*$p < 0.05$, Student's t test). (B) Chromaffin cells expressing Syt-1 or Syt-7 pHluorin were exposed to low-pH (5.5) PSS for ~8-s intervals after an initial 30-s stimulation with 56 mM KCl in the presence of bafilomycin. Low-pH-insensitive events were assumed to have undergone endocytosis and are expressed as percentage of total fusion events. The probability of a fusion event undergoing endocytosis (cavicapture) with Syt-7 (six cells) was significantly different from that with Syt-1 (seven cells; **$p < 0.01$, binomial probability). *P/S* (C) and *P + 2S* (D) lifetimes for individual Syt-1 and Syt-7 fusion events. Syt-1 events are short lived. Only nine of 36 *P/S* increases and one of 23 *P + 2S* changes (increases and decreases) persist for >5 s for Syt-1. In contrast, most Syt-7 fusion events are associated with *P/S* (48 of 51 events) and *P + 2S* (22 of 37 events) changes lasting >5 s.

Ca^{2+} accumulation is commensurate with stimulus intensity (Augustine and Neher, 1992). Changes in stimulus intensity are tied to two different fusion modes for chromaffin cell secretory granules (Fulop *et al.*, 2005). Therefore the goal of the following experiments was to determine whether Syt isoforms were differentially activated by elevations in intracellular Ca^{2+} to promote these different fusion modes. To perform these studies, we first monitored qualitative changes in near-membrane Ca^{2+} in cells transfected with gCaMP5G (Tucker *et al.*, 2003) and exposed to 10, 25, and 56 mM KCl for 50–60 s. The greatest increases in Ca^{2+} were observed with 56 mM KCl. This demonstrates that Ca^{2+} accumulation at the membrane and near fusion sites is sensitive to how strongly the cell is depolarized (Figure 9A). With decreasing amounts of KCl in the depolarizing solution, the $\Delta F/F$ is significantly lower (averaged $\Delta F/F$ data are shown ± SEM). Next we transfected cells with Syt-1–GFP or Syt-7–GFP and monitored whether granules expressing fluorescent isoforms were differentially responsive to KCl depolarization. At the lowest KCl concentration, only a handful of fusion events (seven of 2041 docked granules across 25 cells) were observed for Syt-1, and a similar number (35 of 1994 docked granules across 25 cells) were observed for Syt-7. With a moderate 25 mM KCl stimulation, ~17% of docked Syt-7 granules fused, whereas the number of recorded Syt-1 events remained low. Large numbers of fusion events for Syt-1 were only observed with 56 mM KCl, which also evokes the greatest increases in near-membrane Ca^{2+} (Figure 9, A and B). In fact, the 56 mM stimulation is more effective at activating Syt-1 than Syt-7, with 32% of docked Syt-1 granules fusing as compared with 25% of docked Syt-7 granules. These experiments demonstrate that activation of Syt isoforms is strongly Ca^{2+} dependent. Mild depolarization and small elevations in intracellular Ca^{2+} preferentially trigger Syt-7 granule fusion. Although higher elevations in Ca^{2+} activate both isoforms, it is the Syt-1 granules that fuse with greater frequency.

We further examined the data in Figure 9B to determine whether the time between stimulus application and fusion was different for the two isoforms. As shown in Figure 9, C and D, we separated events into bins, with the first bin constituting events occurring within the first 5 s of the stimulus, the next between 5 and 10 s of the stimulus, and so on. With 25 mM KCl, although the total number of Syt-1 fusion events was small (51 events across 25 cells), ~50% of the granules that fused did so within the first 10 s of the stimulus. Forty percent of Syt-7–GFP granules fused in the same period (Figure 9C). More dramatic effects were observed with 56 mM KCl. With this stimulus, there was a significantly shorter time delay between KCl application and fusion for Syt-1 than Syt-7 in all the bins (Figure 9D). Indeed, almost 80% of Syt-1 granules fused within the first 10 s of the stimulus, compared with only 48% for Syt-7. Only 20% of docked Syt-1 granules fused 10 s or more after the stimulus, compared with 52% of Syt-7 granules. Thus, with a strongly depolarizing stimulus, Syt-1 granules not only fuse more readily than Syt-7 granules, they also tend to fuse earlier.

DISCUSSION

The major findings of this study are that 1) synaptotagmin isoforms Syt-1 and Syt-7 are usually sorted to different secretory granules; 2) the isoforms drive different fusion modes of exocytosis, with Syt-1 favoring rapid and wide fusion pore expansion and Syt-7 slowing or limiting this process; 3) when Syt-1 drives fusion, lumenal and membrane constituents of the granule are released more rapidly and more thoroughly than when Syt-7 granules fuse; and 4) the isoforms are differentially activated by membrane depolarization and concomitant intracellular Ca^{2+} elevations. These results are summarized in Figure 10.

This study began with the surprising observation that in bovine chromaffin cells, unlike PC12 cells (Zhang *et al.*, 2011), there is little colocalization of synaptotagmin isoforms on secretory granules. Even with overexpression, both proteins are detected together on only a fraction of granules screened. A significant functional consequence of isoform segregation is that individual granules are endowed with unique Ca^{2+} sensitivities, allowing for rapid, local control of the fusion mode based on local Ca^{2+} levels. Thereby stimuli that differentially elevate cytosolic Ca^{2+} (Augustine and Neher, 1992; Garcia *et al.*, 2006; Fulop and Smith, 2007; de Diego *et al.*, 2008; Moghadam and Jackson, 2013) can differentially activate granules that will release only some (in the case of Syt-7) or more/all of their contents (in the case of Syt-1). There is consequently a strong Ca^{2+}-dependent component to pore expansion, which may be regulated by the synaptotagmins.

Mild KCl depolarization (25 mM), which moderately elevates intracellular Ca^{2+}, selectively triggers the fusion of docked Syt-7

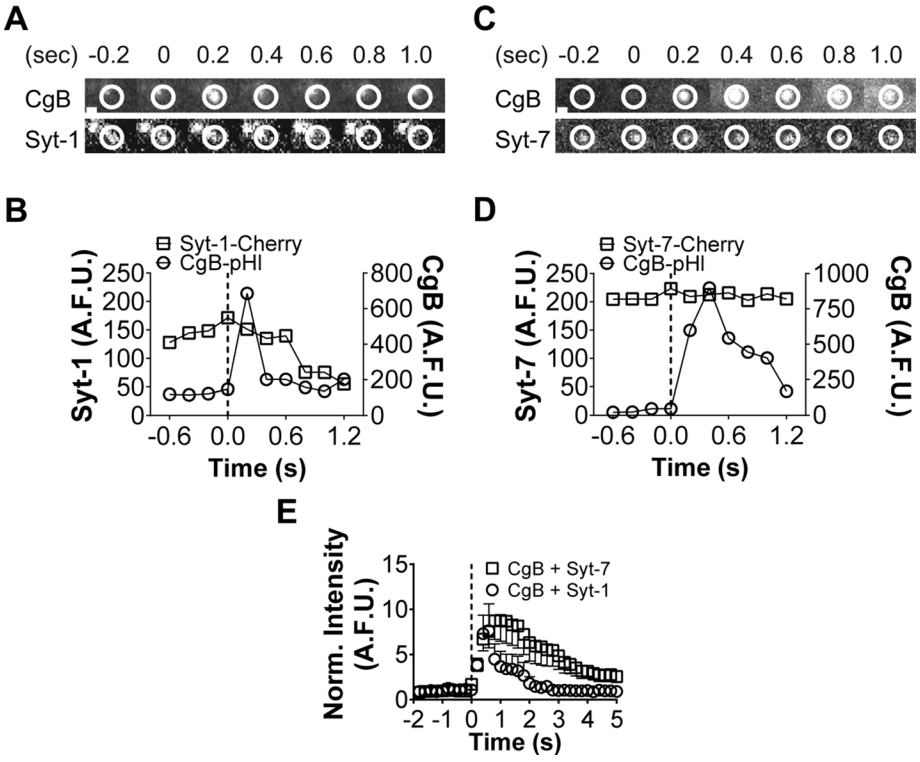

FIGURE 7: Syt-1 granules release lumenal contents more quickly than Syt-7 granules. (A) Fusion of a Syt-1-Cherry granule. CgB-pHluorin intensity increases (indicating fusion) at time 0.2 s (within circled region). Syt-1 and CgB disperse quickly after fusion (dotted line). Note loss of fluorescence within circled region (A, B). (C) Syt-7 remains punctate after fusion (bottom). CgB is released slowly. (D) Graphs for C. (E) On average, CgB is more rapidly released from fusing Syt-1 rather than Syt-7 granules. $n = 19$ for Syt-1 plus CgB; $n = 21$ for Syt-7 plus CgB. After 2 s, averages ± SEM are significantly (*$p < 0.05$) different by Student's t test. Scale bar, 960 nm.

granules (Figure 9B). We define "docked" as a granule resident in the evanescent field for at least 10 s before the stimulus is applied. KCl 56 mM depolarization and correspondingly higher elevations in intracellular Ca^{2+} activate both isoforms but favor fusion of Syt-1 granules. In addition, with this stimulus, differences in the time of isoform activation become apparent. Specifically, the latency between KCl application and fusion is significantly shorter for Syt-1 than Syt-7. Almost 80% of docked Syt-1 granules fuse within 10 s of 56 mM KCl application as opposed to 48% of docked Syt-7 granules during the same period of time (Figure 9D).

Syt-1 and Syt-7 are differentially responsive to the strength of stimulation with varying time courses for activation even in response to the same depolarizing stimulus (56 mM KCl). One therefore wonders whether Syt-1 and Syt-7 are the Ca^{2+} sensors for functionally distinct granule "pools." Such pools are believed to account for the distinct kinetic components of membrane capacitance increases evoked by depolarizing voltage pulses or flash photolysis of Ca^{2+} (Neher and Zucker, 1993; Chow *et al.*, 1994, 1996; Heinemann *et al.*, 1994; Voets *et al.*, 1999; Neher and Sakaba, 2008). The fast kinetic component of the capacitance burst is suggested to reflect an immediately releasable pool (IRP) of granules, which require only mild depolarization for release. Whereas there are important kinetic differences between electrophysiological measurements and imaged secretory responses, the selective activation of Syt-7 in response to mild KCl depolarization is qualitatively consistent with its sorting to the IRP. These granules may be closely localized to Ca^{2+} channels, providing basal catecholamine secretion at a minimal metabolic expense (Voets *et al.*, 1999). With strong depolarization and a higher global change in $[Ca^{2+}]_i$, both Syt-1 and Syt-7 fusion events are observed. Syt-1 granules, however, fuse more readily and fuse earlier than Syt-7 granules (Figure 9, B and D). Thus it is possible that both Syt-1 and Syt-7 granules are found in a ready releasable pool, with differences in their relative distances to Ca^{2+} channels/microdomains accounting for differences in their time courses of activation (Voets *et al.*, 1999).

Despite these similarities, absolute comparisons between electrophysiological and optical measurements are difficult to make for several reasons. For example, differences in release kinetics between the granule pools defined by capacitance are already apparent within tens of milliseconds after depolarization (Horrigan and Bookman, 1994; Voets *et al.*, 1999). This undoubtedly reflects the ability of the electrophysiological approaches to measure early events. In our study, temporal differences in latency to fusion using the high-K^+ stimulation are not apparent for at least 1 s to several seconds (Figure 9, C and D). In addition, the duration of imaged cavicapture events (Figure 4) is slower than the tens of milliseconds–long "stand-alone feet" detected by amperometry (Zhou *et al.*, 1996). Our data may be on the time scale of longer stepwise capacitance changes measured by Lindau and colleagues (Albillos *et al.*, 1997) and "kiss-and-run" events in PC12 cells imaged by Jackson, Chapman, and colleagues (Zhang *et al.*, 2011). The reason for these discrepancies is not clear. An answer will likely require a systematic comparison of optical and electrical measurements in the same group of cells or combinatorial approaches capable, for example, of imaging fusion at the same time as amperometric detection of catecholamine release (Hafez *et al.*, 2005).

Syt-1 and Syt-7 granules diverge not only in their depolarization dependence of activation, but, as noted earlier, in the rate at which they release lumenal and membrane constituents. For instance, Syt-1 releases CgB with more rapid kinetics than Syt-7. Likewise, VMAT-2 is released and spreads along the membrane after fusion of Syt-1 granules, with a diffusion coefficient ($8.92 \pm 1.61 \times 10^{-2}$ μm^2/s, $n = 25$) that is roughly 10 times that of Syt-1 itself. VMAT-2 diffusion out of Syt-7 granules, however, is negligible. The differences in release properties result from the divergent postfusion fates of fused Syt-1 and Syt-7 granules. These fates were monitored with pTIRFM. We previously used dil and polarized excitation light from a 514-nm laser to detect the rapid changes in membrane topology that occur with granule fusion (Anantharam *et al.*, 2010, 2011). In this study, the instrument setup was modified so that a polarized 561-nm beam excited the fluorescence of a different membrane probe—diD. DiD was used because its red-shifted emission spectrum enables two-color imaging studies requiring GFP or pHluorin, which the overlapping emission spectra of dil and GFP/pHluorin all but preclude. Indeed, in earlier studies, two-color imaging was performed with dil and Cerulean (Anantharam *et al.*, 2010). Although brighter than cyan fluorescent protein, Cerulean has a lower extinction coefficient and quantum yield and exhibits decreased pH sensitivity compared

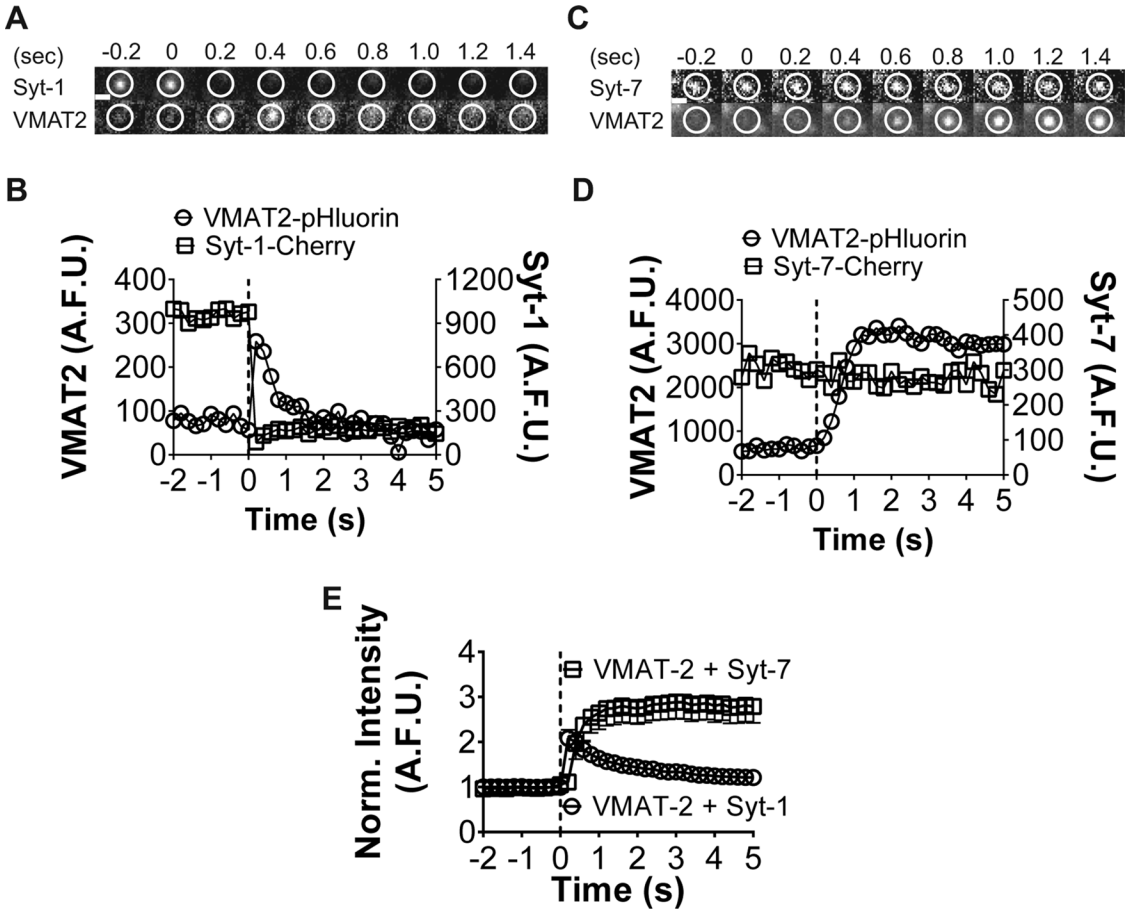

FIGURE 8: A granule membrane protein is released slowly from Syt-7 granules upon fusion. (A) VMAT2-pHluorin fluorescence rapidly disperses from fusing Syt-1 granules (within circled region). (B) Graph for A indicates Syt-1 intensity diminishes after fusion (dotted line), whereas VMAT2 intensity increases and then diminishes. (C, D) VMAT2 movement is restricted from fused Syt-7 granules (D). $n = 24$ for Syt-1 plus VMAT2; $n = 17$ for Syt-7 plus VMAT2. Averages ± SEM are significantly different after 1 s (*$p < 0.05$) by Student's t test. Only negative (–) error bar is shown for VMAT2 plus Syt-7 and positive (+) error bar for VMAT2 plus Syt-1. Scale bar, 960 nm.

with pHluorin or even GFP (Rizzo *et al.*, 2004). Most important, the modification we now introduced makes it possible to extract topological data from fusion events while directly monitoring the recycling kinetics of a protein of interest (e.g., Syt-1, Syt-7, VMAT-2, and CgB). This protein is fused to pHluorin and detects changes in lumenal pH that occur normally during cavicapture (i.e., reacidification) or when a fused granule is experimentally exposed to a low-pH extracellular solution (Anantharam *et al.*, 2010).

Our data show that when Syt-1 drives fusion, the overwhelming outcome is rapid curvature decay of the fused granule/plasma membrane domain. Indeed, 75% (27/36) of Syt-1 events show curvature decay to prefusion levels within 5 s of fusion. The overall probability of endocytosis is accordingly quite low. On the other hand, when Syt-7 drives fusion, indentations representing the fused granule can be remarkably stable. In the majority of cases, they were observed to persist for >80–90 s, the duration of the imaging protocol. Whether the indentation eventually collapses into the plasma membrane or is retrieved via a form of clathrin-dependent endocytosis that occurs at or near the site of fusion (Bittner *et al.*, 2013) was not investigated.

The divergent effects of the isoforms on fusion pore expansion may be a functional consequence of their distinct biochemistry. Syt-1 and Syt-7 exhibit different affinities for Ca^{2+} in the presence of phospholipid membranes. In biochemical assays, the Syt cytoplasmic domains are predicted to vary >10-fold in their $[Ca^{2+}]_{1/2}$ (<1 μM for Syt-7 and 14 μM for Syt-1; Wang *et al.*, 2005). Once bound to Ca^{2+}, the Syts also release membranes with different kinetics (Sugita *et al.*, 2002; Bhalla *et al.*, 2005; Hui *et al.*, 2005). The disassembly of the Syt-1–Ca^{2+}–membrane complex occurs more quickly than disassembly of the Syt-7–Ca^{2+}–membrane complex in membranes containing phosphatidylserine. Thus, when intracellular Ca^{2+} increase to trigger chromaffin cell exocytosis, Syt-7 may insert into and hold the plasma membrane more avidly than Syt-1, thereby stabilizing the fusion pore. The pore would be expected to expand as Syt-7 slowly released the membrane or to reseal as additional proteins (possibly dynamin; Fulop *et al.*, 2008; Chan *et al.*, 2010; Anantharam *et al.*, 2011) are recruited to facilitate fission. In in vitro assays, Syt-1 releases membranes with rapid kinetics. After exocytosis in chromaffin cells, it generally departs the fusion site. It is interesting to note that there is no correlation between the rate of Syt-1 diffusion after fusion and the rate of fusion pore expansion (Supplemental Figure S3E). Once Syt-1 disperses from fusion sites, the underlying granule/plasma membrane domain collapses with a varying time course.

The actions of Syt-7 during secretory granule exocytosis are consistent with its previously reported actions during lysosomal exocytosis in fibroblasts. Lysosomal vesicles remain as puncta after

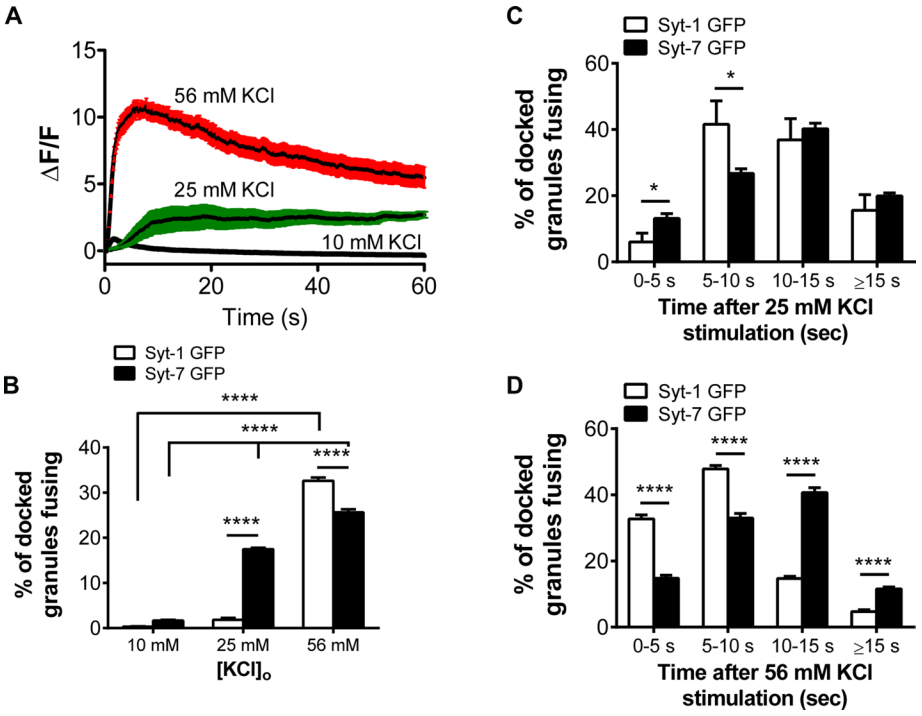

FIGURE 9: Syt-1 and Syt-7 are differentially activated by depolarization. (A) Near-membrane $\Delta F/F$ in cells ($n = 5$, all groups) transfected with gCaMP5G and imaged in TIRF was calculated as described in *Materials and Methods*. Means (solid black lines) of 10 and 25 mM KCl are statistically significant compared with 56 mM KCl (*t* test, ***$p < 0.001$). (B) Syt-1–GFP and Syt-7–GFP were expressed separately in chromaffin cells. The number of fusing Syt-1 or Syt-7 granules for each condition is expressed as a percentage of granules resident in the evanescent field ("docked") at least 10 s before the start of the stimulus. Raw counts of number of events/number of docked granules ($n = 25$ cells for Syt-1 and Syt-7). For Syt-1, 7/2041 (10 mM), 51/2373 (25 mM), and 1089/3273 (56 mM). For Syt-7, 35/1994 (10 mM), 371/2149 (25 mM), and 662/2556 (56 mM). Statistical differences in percentage fusion at 10, 25, and 56 mM KCl (Syt-1 and Syt-7) were assessed with two-way analysis of variance (****$p < 0.0001$). (C, D) The time delay between application of KCl and fusion was calculated for Syt-1– or Syt-7–GFP granules and binned into intervals as indicated. Raw data of number of fusion events in each bin/total number of fusion events. For Syt-1 at 25 mM KCl, 6/51 (0–5 s), 18/51 (5–10 s), 18/51 (10–15 s), and 9/51 (>15 s). For Syt-7 at 25 mM KCl, 48/371 (0–5 s), 99/371 (5–10 s), 150/371 (10–15 s), and 74/371 (>15 s). For Syt-1 at 56 mM KCl, 347/1089 (0–5 s), 529/1089 (5–10 s), 156/1089 (10–15 s), and 57/1089 (>15 s). For Syt-7 at 56 mM KCl, 103/662 (0–5 s), 217/662 (5–10 s), 265/662 (10–15 s), and 77/662 (>15 s). Statistical differences between groups were calculated using the Student's *t* test (*$p < 0.05$; ****$p < 0.0001$).

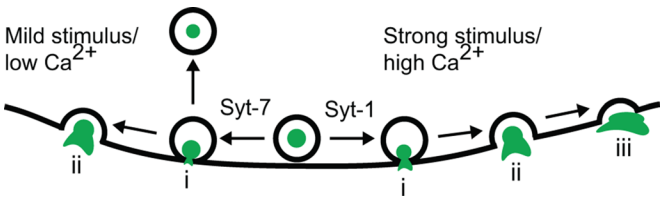

FIGURE 10: On the basis of membrane topological data, measurements of endocytosis, and imaging of lumenal/membrane protein release, we propose that Syt isoforms favor different fusion modes in adrenal chromaffin cells. The isoforms themselves are preferentially activated by mild (Syt-7) and strong (Syt-1) depolarization. Postfusion topologies of Syt-1 granules are consistent with a rapid transition between an initial and wide pore (i → iii), thereby promoting the release of granule lumen and membrane constituents. On the other hand, postfusion topologies of Syt-7 granules indicate a slow transition between an initial and wide pore (i → ii), thereby restricting the release of granule lumen and membrane constituents. In addition, Syt-7 fusion events more frequently result in endocytosis at the site of fusion (i.e., cavicapture) than do Syt-1 events.

fusion, with vesicle membrane collapse only observed when Syt-7 is absent (Chakrabarti *et al.*, 2003; Jaiswal *et al.*, 2004; Andrews and Chakrabarti, 2005). The presence of Syt-7 on fused vesicles prevents the release of large lumenal cargo through the fusion pore or diffusion of membrane proteins along the membrane (Jaiswal *et al.*, 2004). Similarly, in chromaffin cells, the finding that Syt-1 and Syt-7 are rarely found together on granules and favor discrete fusion modes for exocytosis raises the possibility that the postfusion fate of the granule is largely influenced by which isoform it harbors. Alternatively, the Syt isoform may predispose a given granule to fuse under one or another stimulus condition but work together with other regulatory factors to stabilize or destabilize the fusion pore. Considerable evidence has shown that actin dynamics (either disruption or stabilization; Jaiswal *et al.*, 2009), inhibition of myosins (Doreian *et al.*, 2008; Neco *et al.*, 2008; Berberian *et al.*, 2009; Gonzalez-Jamett *et al.*, 2013), inhibition of calcineurin (Engisch and Nowycky, 1998; Sun *et al.*, 2010; Zanin *et al.*, 2013), and disruption of dynamin function by pharmacologic or genetic means (Fulop *et al.*, 2008; Chan *et al.*, 2010; Gonzalez-Jamett *et al.*, 2010, 2013; Anantharam *et al.*, 2011) all alter fusion pore expansion. These elements may be heterogeneously distributed across the cell membrane or preferentially localized to sites of Syt-1 or Syt-7 fusion. The stable or expanding pore may therefore represent a confluence of stimulus-dependent activities of synaptotagmin and other regulators at the fusion site.

Overall, this study provides strong evidence that molecular heterogeneity, rather than homogeneity, may be a defining feature of chromaffin cell secretory granules. Given that this is the case, the obvious question is, to what end? The implication here is that heterogeneity with respect to synaptotagmins provides cells with a tunable, Ca^{2+}-dependent mechanism to control and define the properties of regulated exocytosis. The regulation of the secretory response via synaptotagmin diversity and segregation may also be generalizable to other systems. The design is eminently scalable, so that for cells (e.g., neurons) that receive more complex stimuli, only a greater number of synaptotagmin isoforms is required to regulate release.

MATERIALS AND METHODS

Polarized total internal reflection fluorescence microscopy

Detailed description for the specialized excitation system used to create the orthogonal *p*- and *s*-polarized 561-nm beams and further superimpose them onto the 488-nm beam is provided elsewhere (Anantharam *et al.*, 2010). The system uses Lambda SC smart-shutter controllers (Sutter Instruments, Novato, CA) that allow for rapid selection of three shutter openings sequentially—*p*- and *s*-polarized 561 nm excitation and the 488-nm excitation (one at a time)—and repeats the cycle using MetaMorph software (Molecular Devices,

Sunnyvale, CA). The common beam path was focused through a custom side port to a side-facing filter cube placed below the objective turret of an Olympus IX81 (inverted) microscope (Center Valley, PA) to produce objective-based TIRF illumination. The dichroic mirror/emission filter cube combinations used for the experiments were as follows: z488/561 rpc and z488/561m_TIRF for syt-pHl/ DiD or CgB pHl/syt-Cherry imaging and z488/640 rpc and z488/640m for imaging antibody staining in TIRF (Chroma Technology, Brattleboro, VT). For directing the incident beam at ~70° from the normal on the coverslip, the beam was focused on the periphery of the back focal plane of a 60×/1.49 numerical aperture (NA) oil immersion objective (Olympus), thereby giving a decay constant for the evanescent field of ~110 nm.

Two additional lenses (1.6× and 2×) in the emission path between the microscope and electron-multiplying charge-coupled device (EM CCD) camera give a final pixel size of ~80 nm. Images were acquired using a cooled EM CCD camera (iXon3, Andor Technology, South Windsor, CT). The acquisition of the digital image was in synchrony with the opening of the smart shutters specific for the individual beams. The images were acquired at ~5 Hz with 25-ms exposures and 300 gain (EM setting). One complete cycle of three exposures lasted ~200 ms.

Chromaffin cell preparation and transfection

The chromaffin cells were isolated from bovine adrenal medulla, and transient transfections were performed as described earlier (Wick *et al.*, 1993). To facilitate cell adhesion, cells were plated on 35-mm tissue culture dishes with cover glass bottom (refractive index, 1.51; World Precision Instruments, Sarasota, FL) precoated with poly-D-lysine and bovine collagen. Cells were transiently transfected by electroporation with plasmid(s) using the Neon transfection system (Invitrogen, Carlsbad, CA). The procedure for electroporation was standardized, and the cells were transfected with a single pulse of 1100 mV for a period of 40 ms. The Syt-1–pHluorin and Syt-7xpHluorin constructs in pCI vector were transfected alone in DiD experiments. The Syt-1–Cherry and Syt-7–Cherry constructs were cotransfected with CgB-pHluorin or VMAT2-pHluorin. The VMAT2-pHluorin plasmid was a gift from Robert Edwards (University of California, San Francisco, San Francisco, CA). Syt isoform sorting was determined in two ways: 1) expression of NPY-Cer alone, followed by immunocytochemistry using antibodies toward the Syt isoforms; or 2) cotransfection of Syt-1–Cherry, Syt-7–GFP, and NPY-Cer. The parent NPY plasmid was a gift from Wolfhard Almers (Vollum Institute, Oregon Health and Science University, Portland, OR). Stimulation-evoked surface distribution was visualized by TIRF microscopy of cells by coexpression of Syt-1–WT and myc-tagged Syt-7 (gift of Thomas Sudhof, Stanford University, Palo Alto, CA) with immunocytochemistry. All experiments were performed 2–5 d after transfection.

Cell stimulation

Before imaging, cells were stained with diD added directly to cells bathed in PSS at 1:200 dilution. The cells were quickly washed several times in PSS to get rid of the excessive dye and then used immediately. All TIRF experiments were performed in PSS containing 145 mM NaCl, 5.6 mM KCl, 2.2 mM $CaCl_2$, 0.5 mM $MgCl_2$, 5.6 mM glucose, and 15 mM 4-(2-hydroxyethyl)-1-piperazineethanesulfonic acid (HEPES), pH 7.4. A computer-controlled perfusion system, ALA-VM4 (ALA Scientific Instruments, Westbury, NY), was used to perfuse individual cells with a needle (100-µm inner diameter) under positive pressure. Normally, cells were perfused with PSS for 10 s and then stimulated with high-K^+-containing solution to secrete (95 mM NaCl, 56 mM KCl, 5 mM $CaCl_2$, 0.5 mM $MgCl_2$, 5.6 mM glucose, 15 mM HEPES, pH 7.4) for ~60 s to trigger exocytosis. Endocytosis was measured as previously described (Anantharam *et al.*, 2011). Briefly, cells were first perfused with elevated-K^+ PSS at pH 7.4 for 30 s and then exposed to pH 5.5 PSS (HEPES was substituted by 2-(*N*-morpholino)ethanesulfonic acid buffer) to quench the fluorescence of any extracellular facing pHl. The cells were then again exposed to normal PSS at pH 7.4, and the cycle was repeated every 10 s. Bafilomycin (Santa Cruz Biotechnology, Santa Cruz, CA), an inhibitor of vacuolar-type H^+-ATPase that reacidifies endocytosed granules, was added to PSS at a final concentration of 5 µM. Experiments were performed at ambient temperatures of 30–32°C.

Image analysis

The Syt-pHluorin, diD *s*- and *p*-polarization emission images were captured sequentially using MetaMorph software. The *P/S* and *P + 2S* ratios were calculated after normalization on a pixel-to-pixel basis for every image, and custom software written in IDL (ITT, Boulder, CO) was used to align the transformations to the Syt-pHluorin images. Individual granules undergoing exocytosis were evident by increase in the pHluorin intensity after fusion with the plasma membrane as a result of change in pH of the granule. The *P/S* and *P + 2S* changes were calculated by centering the region of interest over localized increase in *P/S* ratio at the site of exocytosis in a radius of ~240 nm.

Multiple factors, such as relative intensities of the *p*- and *s*-polarized excitations, biases in optical system, and certain interference fringes, can result in variations in the *P/S* ratio. To reduce this discrepancy and further allow for a theoretical comparison, a solution of 10 mM rhodamine 6G (Invitrogen), a dye predicted to be randomly oriented, was used to normalize the *P/S* data from DiD emission. The spatial mean of rhodamine 6G emission excited by each of the *p*- and *s*-polarized 561-nm beams was used for normalization of data. Similarly, for correcting the *P + 2S* values, the amplitudes of *p* relative to *s* were calculated by calibration of rhodamine 6G. Topological changes were considered significant if *P/S* and *P + 2S* increased above 7% (3× SD of the mean) with respect to baseline within five frames of the fusion event (indicated by pHluorin or GFP intensity changes). Emission intensity changes that did not cross the 7% threshold were not included in the data set for analysis.

The average fluorescence change of gCaMP5G in response to different depolarizing stimuli (10, 25, and 56 mM KCl) was estimated not as $[Ca^{2+}]$, but as the pseudoratio $\Delta F/F = (F - F_{base})/(F_{base} - B)$, where F is the measured fluorescence intensity of the genetically encoded Ca^{2+} indicator, F_{base} the fluorescence intensity of the Ca^{2+} indicator in the cell before stimulation, and B the background signal determined from the average of areas adjacent to the cell.

Immunocytochemistry

For immunofluorescence microscopy to detect synaptotagmin isoform distribution in cells expressing NPY Cerulean, isolated chromaffin cells on the glass cover dish were fixed with 4% paraformaldehyde in phosphate-buffered saline (PBS) for 30 min. The cells were then rinsed and quenched with 50 mM NH_4Cl in PBS. After washing, the cell membrane was permeabilized for 7 min with acetone to preserve the cell cytoskeleton. The cells were further washed with Tris-buffered saline (TBS) and blocked with 1% gelatin in TBS and 4% donkey serum for 30 min each. Primary and secondary antibodies were diluted in a solution of 2–4 mg/ml BSA. Cells were incubated for 2 h at room temperature with a combination of the following antibodies: monoclonal anti–Syt-1 antibody (antibody 41.1) and polyclonal anti-Syt-7 antibody (Synaptic Systems, Göttingen, Germany). The cells were then washed five times in TBS and incubated for 70 min with Alexa-conjugated anti-rabbit and anti-mouse

secondary antibodies (Molecular Probes/Invitrogen, Eugene, OR). The cells were washed five times after the incubation and imaged by confocal microscopy.

Alternatively, to visualize the stimulation-evoked surface distribution of the Syt isoforms, the cells expressing Syt-1 WT and myc-tagged Syt-7 were first washed with PSS at room temperature, followed by stimulation with either a high-K^+-containing PSS solution (56 mM KCl) or low-K^+-containing PSS solution (10 mM KCl) for 1 min at room temperature. All activity within the cell after stimulation was arrested using cold PSS. The cells were further incubated with the following antibodies for 2 h on ice (4°C): monoclonal anti–Syt-1 antibody and myc-tag antibody for Syt-7 (Cell Signaling Technology, Danvers, MA). The cells were washed five times with TBS and then fixed at 37°C using the procedure described. After blocking, the cells were stained by incubation with Alexa-conjugated anti-rabbit and anti-mouse secondary antibodies (Molecular Probes/Invitrogen) for 70 min at room temperature as previously described.

Confocal microscopy

For transfected and immunostained cells showing a fluorescence signal, images were acquired on a Leica TCS SP5 confocal microscope with a 63×/1.40 NA oil objective. For imaging, a 405-nm diode laser, an argon 488-nm laser, and a HeNe red 594-nm laser were used. The images obtained were analyzed with ImageJ software (National Institutes of Health, Bethesda, MD). Statistical calculations were performed using Prism 6 software (GraphPad, La Jolla, CA).

ACKNOWLEDGMENTS

We thank Ronald W. Holz, Daniel Axelrod, and Mary Bittner for helpful suggestions on all aspects of this study. We also thank James T. Taylor, Johan Edvinsson, Rachel L. Aikman, and Praneeth Katrapati for technical assistance. This research was supported by National Institutes of Health Grant MH 61876 (to E.R.C.), American Heart Association Grant 13SDG14420049, and start-up funds from Wayne State University (to A.A.).

REFERENCES

Albillos A, Dernick G, Horstmann H, Almers W, Alvarez de Toledo G, Lindau M (1997). The exocytotic event in chromaffin cells revealed by patch amperometry. Nature 389, 509–512.

Allersma MW, Wang L, Axelrod D, Holz RW (2004). Visualization of regulated exocytosis with a granule-membrane probe using total internal reflection microscopy. Mol Biol Cell 15, 4658–4668.

Anantharam A, Bittner MA, Aikman RL, Stuenkel EL, Schmid SL, Axelrod D, Holz RW (2011). A new role for the dynamin GTPase in the regulation of fusion pore expansion. Mol Biol Cell 22, 1907–1918.

Anantharam A, Onoa B, Edwards RH, Holz RW, Axelrod D (2010). Localized topological changes of the plasma membrane upon exocytosis visualized by polarized TIRFM. J Cell Biol 188, 415–428.

Andrews NW, Chakrabarti S (2005). There's more to life than neurotransmission: the regulation of exocytosis by synaptotagmin VII. Trends Cell Biol 15, 626–631.

Augustine GJ, Neher E (1992). Calcium requirements for secretion in bovine chromaffin cells. J Physiol 450, 247–271.

Bai J, Wang CT, Richards DA, Jackson MB, Chapman ER (2004). Fusion pore dynamics are regulated by synaptotagmin*t-SNARE interactions. Neuron 41, 929–942.

Berberian K, Torres AJ, Fang Q, Kisler K, Lindau M (2009). F-actin and myosin II accelerate catecholamine release from chromaffin granules. J Neurosci 29, 863–870.

Bhalla A, Tucker WC, Chapman ER (2005). Synaptotagmin isoforms couple distinct ranges of Ca2+, Ba2+, and Sr2+ concentration to SNARE-mediated membrane fusion. Mol Biol Cell 16, 4755–4764.

Bittner MA, Aikman RL, Holz RW (2013). A nibbling mechanism for clathrin-mediated retrieval of secretory granule membrane after exocytosis. J Biol Chem 288, 9177–9188.

Brose N, Petrenko AG, Südhof TC, Jahn R (1992). Synaptotagmin: a calcium sensor on the synaptic vesicle surface. Science 256, 1021–1025.

Chakrabarti S, Kobayashi KS, Flavell RA, Marks CB, Miyake K, Liston DR, Fowler KT, Gorelick FS, Andrews NW (2003). Impaired membrane resealing and autoimmune myositis in synaptotagmin VII-deficient mice. J Cell Biol 162, 543–549.

Chan SA, Doreian B, Smith C (2010). Dynamin and myosin regulate differential exocytosis from mouse adrenal chromaffin cells. Cell Mol Neurobiol 30, 1351–1357.

Chow RH, Klingauf J, Heinemann C, Zucker RS, Neher E (1996). Mechanisms determining the time course of secretion in neuroendocrine cells. Neuron 16, 369–376.

Chow RH, Klingauf J, Neher E (1994). Time course of Ca2+ concentration triggering exocytosis in neuroendocrine cells. Proc Natl Acad Sci USA 91, 12765–12769.

Damase-Michel C, Tavernier G, Giraud P, Montastruc JL, Montastruc P, Tran MA (1993). Effects of clonidine, dihydralazine and splanchnic nerve stimulation on the release of neuropeptide Y, MET-enkephalin and catecholamines from dog adrenal medulla. Naunyn-Schmiedeberg's Arch Pharmacol 348, 379–384.

de Diego AM, Gandia L, Garcia AG (2008). A physiological view of the central and peripheral mechanisms that regulate the release of catecholamines at the adrenal medulla. Acta Physiol (Oxf) 192, 287–301.

Doreian BW, Fulop TG, Smith CB (2008). Myosin II activation and actin reorganization regulate the mode of quantal exocytosis in mouse adrenal chromaffin cells. J Neurosci 28, 4470–4478.

Edwards AV, Jones CT (1993). Autonomic control of adrenal function. J Anat 183, 291–307.

Engisch KL, Nowycky MC (1998). Compensatory and excess retrieval: two types of endocytosis following single step depolarizations in bovine adrenal chromaffin cells. J Physiol 506, 591–608.

Fukuda M (2004). RNA interference-mediated silencing of synaptotagmin IX, but not synaptotagmin I, inhibits dense-core vesicle exocytosis in PC12 cells. Biochem J 380, 875–879.

Fukuda M, Kanno E, Satoh M, Saegusa C, Yamamoto A (2004). Synaptotagmin VII Is targeted to dense-core vesicles and regulates their Ca2+-dependent exocytosis in PC12 cells. J Biol Chem 279, 52677–52684.

Fukuda M, Kowalchyk JA, Zhang X, Martin TFJ, Mikoshiba K (2002). Synaptotagmin IX regulates Ca2+-dependent secretion in PC12 cells. J Biol Chem 277, 4601–4604.

Fulop T, Doreian B, Smith C (2008). Dynamin I plays dual roles in the activity-dependent shift in exocytic mode in mouse adrenal chromaffin cells. Arch Biochem Biophys 477, 146–154.

Fulop T, Smith C (2007). Matching native electrical stimulation by graded chemical stimulation in isolated mouse adrenal chromaffin cells. J Neurosci Methods 166, 195–202.

Fulop T, Radabaugh S, Smith C (2005). Activity-dependent differential transmitter release in mouse adrenal chromaffin cells. J Neurosci 25, 7324–7332.

Garcia AG, Garcia-De-Diego AM, Gandia L, Borges R, Garcia-Sancho J (2006). Calcium signaling and exocytosis in adrenal chromaffin cells. Physiol Rev 86, 1093–1131.

Gonzalez-Jamett AM, Baez-Matus X, Hevia MA, Guerra MJ, Olivares MJ, Martinez AD, Neely A, Cardenas AM (2010). The association of dynamin with synaptophysin regulates quantal size and duration of exocytotic events in chromaffin cells. J Neurosci 30, 10683–10691.

Gonzalez-Jamett AM *et al.* (2013). Dynamin-2 regulates fusion pore expansion and quantal release through a mechanism that involves actin dynamics in neuroendocrine chromaffin cells. PLoS One 8, e70638.

Hafez I, Kisler K, Berberian K, Dernick G, Valero V, Yong MG, Craighead HG, Lindau M (2005). Electrochemical imaging of fusion pore openings by electrochemical detector arrays. Proc Natl Acad Sci USA 102, 13879–13884.

Heinemann C, Chow RH, Neher E, Zucker RS (1994). Kinetics of the secretory response in bovine chromaffin cells following flash photolysis of caged Ca2+. Biophys J 67, 2546–2557.

Horrigan FT, Bookman RJ (1994). Releasable pools and the kinetics of exocytosis in adrenal chromaffin cells. Neuron 13, 1119–1129.

Hui E, Bai J, Wang P, Sugimori M, Llinas RR, Chapman ER (2005). Three distinct kinetic groupings of the synaptotagmin family: candidate sensors for rapid and delayed exocytosis. Proc Natl Acad Sci USA 102, 5210–5214.

Jaiswal JK, Chakrabarti S, Andrews NW, Simon SM (2004). Synaptotagmin VII restricts fusion pore expansion during lysosomal exocytosis. PLoS Biol 2, E233.

Jaiswal JK, Rivera VM, Simon SM (2009). Exocytosis of post-Golgi vesicles is regulated by components of the endocytic machinery. Cell 137, 1308–1319.
Lynch KL, Martin TFJ (2007). Synaptotagmins I and IX function redundantly in regulated exocytosis but not endocytosis in PC12 cells. J Cell Sci 120, 617–627.
Moghadam PK, Jackson MB (2013). The functional significance of synaptotagmin diversity in neuroendocrine secretion. Front Endocrinol 4, 124.
Neco P, Fernandez-Peruchena C, Navas S, Lindau M, Gutierrez LM, Alvarez de Toledo G, Ales E (2008). Myosin II contributes to fusion pore expansion during exocytosis. J Biol Chem 283, 10949–10957.
Neher E, Sakaba T (2008). Multiple roles of calcium ions in the regulation of neurotransmitter release. Neuron 59, 861–872.
Neher E, Zucker RS (1993). Multiple calcium-dependent processes related to secretion in bovine chromaffin cells. Neuron 10, 21–30.
Perrais D, Kleppe IC, Taraska JW, Almers W (2004). Recapture after exocytosis causes differential retention of protein in granules of bovine chromaffin cells. J Physiol Online 560, 413–428.
Rizzo MA, Springer GH, Granada B, Piston DW (2004). An improved cyan fluorescent protein variant useful for FRET. Nat Struct Biol 22, 445–449.
Schonn JS, Maximov A, Lao Y, Sudhof TC, Sorensen JB (2008). Synaptotagmin-1 and -7 are functionally overlapping Ca2+ sensors for exocytosis in adrenal chromaffin cells. Proc Natl Acad Sci USA 105, 3998–4003.
Sugita S, Shin OH, Han W, Lao Y, Sudhof TC (2002). Synaptotagmins form a hierarchy of exocytotic Ca(2+) sensors with distinct Ca(2+) affinities. EMBO J 21, 270–280.
Sun T *et al*. (2010). The role of calcium/calmodulin-activated calcineurin in rapid and slow endocytosis at central synapses. J Neurosci 30, 11838–11847.
Taraska JW, Almers W (2004). Bilayers merge even when exocytosis is transient. Proc Natl Acad Sci USA 101, 8780–8785.
Taraska JW, Perrais D, Ohara-Imaizumi M, Nagamatsu S, Almers W (2003). Secretory granules are recaptured largely intact after stimulated exocytosis in cultured endocrine cells. Proc Natl Acad Sci USA 100, 2070–2075.
Tucker WC, Edwardson JM, Bai J, Kim HJ, Martin TF, Chapman ER (2003). Identification of synaptotagmin effectors via acute inhibition of secretion from cracked PC12 cells. J Cell Biol 162, 199–209.
Tucker WC, Weber T, Chapman ER (2004). Reconstitution of Ca2+-regulated membrane fusion by synaptotagmin and SNAREs. Science 304, 435–438.
Voets T, Moser T, Lund PE, Chow RH, Geppert M, Sudhof TC, Neher E (2001). Intracellular calcium dependence of large dense-core vesicle exocytosis in the absence of synaptotagmin I. Proc Natl Acad Sci USA 98, 11680–11685.
Voets T, Neher E, Moser T (1999). Mechanisms underlying phasic and sustained secretion in chromaffin cells from mouse adrenal slices. Neuron 23, 607–615.
Wang CT, Bai J, Chang PY, Chapman ER, Jackson MB (2006). Synaptotagmin-Ca2+ triggers two sequential steps in regulated exocytosis in rat PC12 cells: fusion pore opening and fusion pore dilation. J Physiol 570, 295–307.
Wang CT, Grishanin R, Earles CA, Chang PY, Martin TFJ, Chapman ER, Jackson MB (2001). Synaptotagmin modulation of fusion pore kinetics in regulated exocytosis of dense-core vesicles. Science 294, 1111–1115.
Wang CT, Lu JC, Bai J, Chang PY, Martin TF, Chapman ER, Jackson MB (2003). Different domains of synaptotagmin control the choice between kiss-and-run and full fusion. Nature 424, 943–947.
Wang P, Chicka MC, Bhalla A, Richards DA, Chapman ER (2005). Synaptotagmin VII is targeted to secretory organelles in PC12 cells, where it functions as a high-affinity calcium sensor. Mol Cell Biol 25, 8693–8702.
Wick PW, Senter RA, Parsels LA, Holz RW (1993). Transient transfection studies of secretion in bovine chromaffin cells and PC12 cells: generation of kainate-sensitive chromaffin cells. J Biol Chem 268, 10983–10989.
Zanin MP, Mackenzie KD, Peiris H, Pritchard MA, Keating DJ (2013). RCAN1 regulates vesicle recycling and quantal release kinetics via effects on calcineurin activity. J Neurochem 124, 290–299.
Zhang Z, Wu Y, Wang Z, Dunning FM, Rehfuss J, Ramanan D, Chapman ER, Jackson MB (2011). Release mode of large and small dense-core vesicles specified by different synaptotagmin isoforms in PC12 cells. Mol Biol Cell 22, 2324–2336.
Zhou Z, Misler S, Chow RH (1996). Rapid fluctuations in transmitter release from single vesicles in bovine adrenal chromaffin cells. Biophys J 70, 1543–1552.